Cell Host & Microbe
Article

DC-SIGN as a Receptor for Phleboviruses

Pierre-Yves Lozach,[1,*] Andreas Kühbacher,[1,3] Roger Meier,[1] Roberta Mancini,[1] David Bitto,[1,4] Michèle Bouloy,[2] and Ari Helenius[1,*]
[1]Institute of Biochemistry, ETH Zurich, Schafmattstrasse 18, CH-8093 Zurich, Switzerland
[2]Unité de Génétique Moléculaire des Bunyavirus, Institut Pasteur, 25 rue du Dr Roux, 75015 Paris, France
[3]Present address: Unité Interactions Bactéries-Cellules, Institut Pasteur, 25 rue du Dr Roux, 75015 Paris, France
[4]Present address: Particle Imaging Centre, University of Oxford, Roosevelt Drive, Oxford OX3 7BN, UK
*Correspondence: lozach@bc.biol.ethz.ch (P.-Y.L.), ari.helenius@bc.biol.ethz.ch (A.H.)
DOI 10.1016/j.chom.2011.06.007

SUMMARY

During natural transmission, bunyaviruses are introduced into the skin through arthropod bites, and dermal dendritic cells (DCs) are the first to encounter incoming viruses. DC-SIGN is a C-type lectin highly expressed on the surface of dermal DCs. We found that several arthropod-borne phleboviruses (*Bunyaviridae*), including Rift Valley fever and Uukuniemi viruses, exploit DC-SIGN to infect DCs and other DC-SIGN-expressing cells. DC-SIGN binds the virus directly via interactions with high-mannose *N*-glycans on the viral glycoproteins and is required for virus internalization and infection. In live cells, virus-induced clustering of cell surface DC-SIGN could be visualized. An endocytosis-defective mutant of DC-SIGN was unable to mediate virus uptake, indicating that DC-SIGN is an authentic receptor required for both attachment and endocytosis. After internalization, viruses separated from DC-SIGN and underwent trafficking to late endosomes. Our study provides real-time visualization of virus-receptor interactions on the cell surface and establishes DC-SIGN as a phlebovirus entry receptor.

INTRODUCTION

The *Bunyaviridae* family comprises five genera (*Hantavirus, Nairovirus*, *Orthobunyavirus*, *Phlebovirus*, and *Tospovirus*) with more than 350 members worldwide (Schmaljohn and Nichol, 2007). Many cause severe illness in humans, such as encephalitis and hemorrhagic fever. With the exception of hantaviruses, bunyaviruses are spread by hematophagous arthropods such as mosquitoes and ticks, i.e., they are *ar*thropod-*bo*rne viruses (arboviruses). With an increasing number of outbreaks, bunyaviruses are considered emerging agents of diseases (Soldan and González-Scarano, 2005).

Bunyavirus particles are enveloped and spherical with a diameter of about 100 nm. The negative-sense RNA genome has three segments present in the form of pseudo-helical ribonucleoproteins (RNPs) (Schmaljohn and Nichol, 2007). The RNA segments replicate in the cytosol and encode four structural proteins: the nucleoprotein N, the RNA-dependent RNA polymerase, and two transmembrane glycoproteins (G_N and G_C). Protein N is associated with the RNA genome and, together with the viral polymerase, forms the RNPs. In the envelope, the glycoproteins form spike-like projections responsible for virus attachment to host cells and for penetration by membrane fusion (Lozach et al., 2010; Overby et al., 2008).

Transmission, tropism, receptors, and cell entry remain poorly characterized. While hantaviruses have been shown to use β3 integrin to enter endothelial cells (Gavrilovskaya et al., 1998), it is not known whether the integrin serves as a receptor or attachment factor. After binding, bunyavirus penetration depends on endocytic internalization and acidification in late endosomes (LEs) (Lozach et al., 2010).

During natural transmission, bunyaviruses are introduced into the skin through bites by infected arthropods. Due to their presence in the anatomical site of initial infection, dermal dendritic cells (DCs) are among the first cells to encounter the incoming viruses. Dermal DCs specifically express on their surface DC-specific intercellular adhesion molecule 3-grabbing nonintegrin (DC-SIGN), a C-type (calcium-dependent) lectin specialized for the capture and presentation of foreign antigens (van Kooyk, 2008).

DC-SIGN is a type II membrane protein that binds high-mannose *N*-glycans through its C-terminal carbohydrate recognition domain (CRD) (Svajger et al., 2010). It is present on the cell surface in different oligomerization states with homotetramers having the highest avidity for substrates (Svajger et al., 2010). Since high-mannose *N*-glycans are typical for insect-derived glycoproteins, interactions between DC-SIGN and arboviruses are thought to be particularly relevant. Alpha- and flaviviruses have indeed been shown to depend on DC-SIGN to infect immature DCs (Svajger et al., 2010). A direct role of DC-SIGN in virus internalization beyond attachment has, however, not been demonstrated.

To determine whether DCs support bunyavirus infection and whether DC-SIGN is involved, we analyzed virus binding, internalization, and membrane trafficking of various phleboviruses in DC-SIGN-expressing cell systems. The results provide a detailed picture of virus-DC-SIGN interaction and establish a role for DC-SIGN as a receptor for viral endocytosis and infection.

RESULTS

Rift Valley Fever and Uukuniemi Viruses infect DCs

Immature DCs were generated from human peripheral blood mononuclear cells (PBMCs). To determine whether they supported infection by bunyaviruses, we tested two phleboviruses,

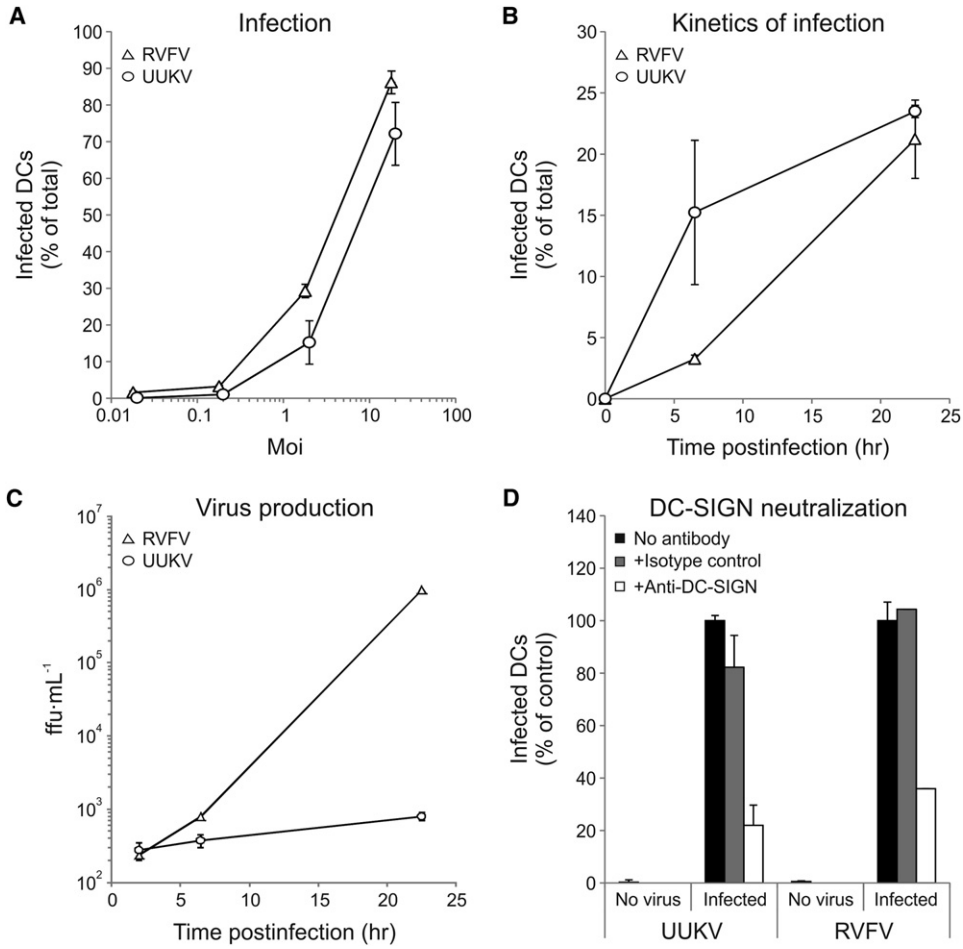

Figure 1. DC-SIGN Mediates Infection of DCs by RVFV and UUKV

(A) Monocyte-derived DCs were infected with RVFV and UUKV and intracellular expression of viral proteins detected by FACS analysis 7 hr later. Infection is expressed as the percentage of viral protein-positive cells (percent of total). Error bars represent the standard deviation (SD).

(B) RVFV and UUKV infection (moi of 0.2 and 2, respectively) was monitored in DCs over 24 hr as described above. Error bars represent the SD.

(C) Supernatants of DCs challenged with RVFV and UUKV (moi of 0.02 and 0.2, respectively) were assessed over 24 hr for the production of viral progeny. Titers were determined by plaque assay and expressed as focus-forming units (ffu) per ml. Error bars represent the SD.

(D) DCs were infected with RVFV and UUKV (moi ~2) in the presence of the anti-DC-SIGN mAb 1621 or an isotype control IgG2a (25 $\mu g \cdot ml^{-1}$). Infection was quantified by FACS 7 hr later and normalized to infection in the absence of Abs (% of control). Error bars represent the SD.

the Rift Valley fever (RVFV) and Uukuniemi (UUKV) viruses. Immature DCs were exposed to these viruses for 7 hr and immunostained with antibodies (Abs) against the protein N of RVFV or UUKV. A fluorescence-activated cell sorter (FACS) allowed quantitative detection of infected cells. More than 70% of cells were infected at the highest multiplicity of infection (moi) (Figure 1A). The fraction of infected cells increased over time (Figure 1B), showing that the signal detected corresponded to viral replication and not to input particles. Titration of cell-free supernatants, collected from challenged DCs, indicated that large amounts of infectious RVFV progeny were released within 24 hr postinfection. In contrast, although the cells were infected, the production of infectious UUKV particles was minimal (Figure 1C).

DC-SIGN Mediates Infection

To examine the role of DC-SIGN in the infection of DCs, we tested infection in the presence of a monoclonal Ab (mAb 1621) against the lectin. Infection by RVFV and UUKV was reduced by 70%–80% but was unaffected by isotype control mAbs (Figure 1D).

The capacity of DC-SIGN to promote infection was confirmed using Raji cells stably expressing DC-SIGN (Raji-DC-SIGN) after transduction with a TRIPΔU3 lentiviral vector encoding human DC-SIGN (Lozach et al., 2005). Raji cells are normally poorly infected by phleboviruses, or not at all. As expected, parental Raji cells were not infected with RVFV, UUKV, or two additional phleboviruses, Punta Toro (PTV) and Toscana (TOSV), at a moi of 1 or less, and only marginally with RVFV and PTV at higher moi (Figures 2A and 2B). However, when DC-SIGN was expressed, a significant fraction of cells was infected at a moi of 1.

Similarly, infection of HeLa and Vero cells with UUKV at various moi was dramatically increased when the lectin was expressed (Figure 2B). That the fraction of DC-SIGN-expressing HeLa (HeLa-DC-SIGN) cells infected increased over time, and

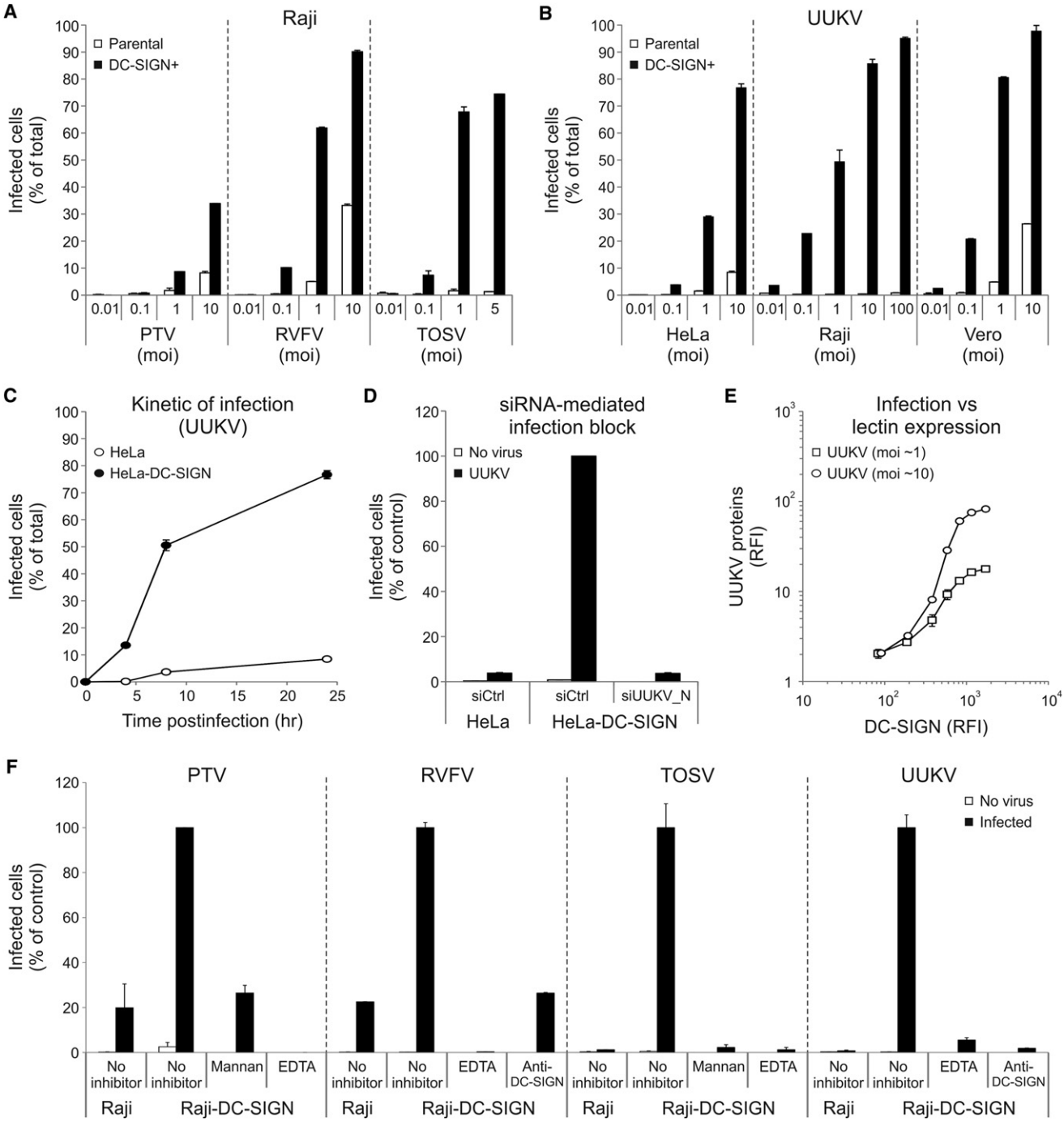

Figure 2. DC-SIGN Ectopic Expression Enhances Phlebovirus Infection

(A) Parental and DC-SIGN-expressing Raji cells were infected with phleboviruses (RVFV, PTV, and TOSV) and infection analyzed by FACS 18 hr later. Error bars represent the SD.

(B) Parental and DC-SIGN-expressing HeLa, Raji, and Vero cells were infected with UUKV and infection quantified 18 hr later. Error bars represent the SD.

(C) UUKV infection (moi ~10) was monitored over 24 hr in parental and DC-SIGN-expressing HeLa (HeLa-DC-SIGN) cells by FACS analysis. Error bars represent the SD.

(D) HeLa-DC-SIGN cells treated with an UUKV nucleoprotein N siRNA (siUUKV_N) were infected with UUKV (moi ~2.5). Infection was quantified by FACS 7 hr later and normalized to number and infection of HeLa-DC-SIGN cells treated with a negative-control siRNA (siCtrl). Error bars represent the SD.

(E) DC-SIGN-expressing Raji cells were infected with UUKV and harvested 7 hr later. UUKV proteins and DC-SIGN expression are expressed as the relative fluorescence intensities (RFI) measured by FACS. Error bars represent the SD.

(F) DC-SIGN-expressing Raji (Raji-DC-SIGN) cells were infected with PTV, RVFV, and TOSV (moi ~1) or UUKV (moi ~5) in the presence of inhibitors blocking DC-SIGN such as mannan (20 $\mu g \cdot ml^{-1}$), EDTA (5 mM), and anti-DC-SIGN mAb 1621 (25 $\mu g \cdot ml^{-1}$). Infection was determined by FACS 18 hr later and normalized to infection of Raji-DC-SIGN cells in the absence of inhibitors. Error bars represent the SD.

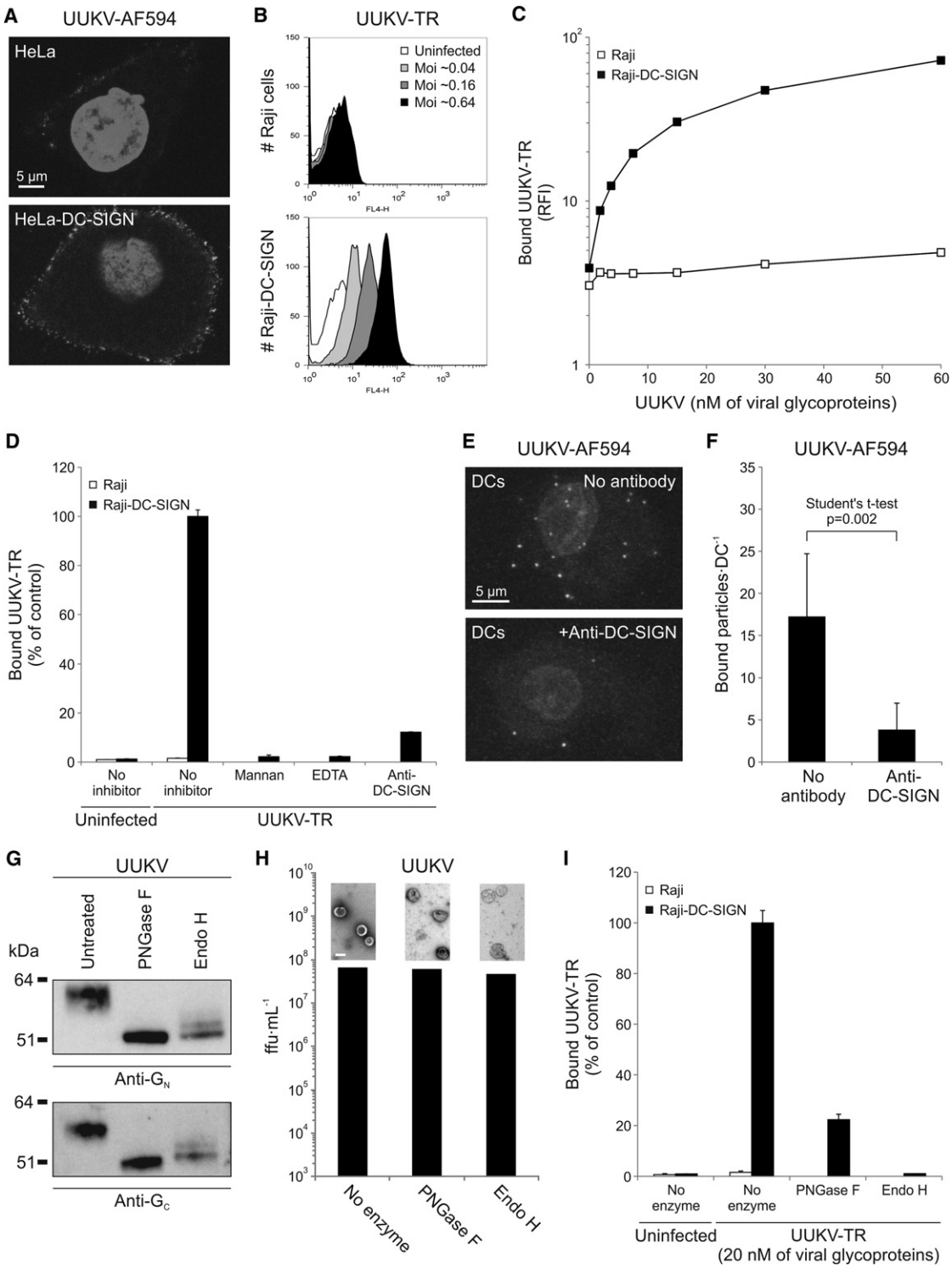

Figure 3. High-Mannose Oligosaccharides on Viral Glycoproteins Are Responsible for UUKV Binding to DC-SIGN

(A) Fluorescent UUKV particles (UUKV-AF594) were bound to HeLa and HeLa-DC-SIGN (moi ~5) for 1 hr on ice before fixation and imaging with confocal microscope. Spots are cell-associated virus particles seen in one focal plane. Nuclei were stained with DRAQ5.

(B) Varying amounts of fluorescent UUKV particles (UUKV-TR) were bound to Raji and Raji-DC-SIGN cells for 1 hr on ice before fixation and FACS analysis.

(C) Serial dilutions of UUKV-TR were bound to Raji and Raji-DC-SIGN cells on ice. UUKV-TR inputs were normalized according to the concentration of viral glycoproteins. Virus binding is expressed as the cell-associated RFI measured by FACS. Error bars represent the SD (not visible on the graph).

(D) UUKV-TR was bound to Raji-DC-SIGN cells (moi ~0.25) on ice in the presence of the DC-SIGN inhibitors described in Figure 2F. Binding was quantified by FACS and normalized to binding to Raji-DC-SIGN cells in the absence of inhibitors. Error bars represent the SD.

that the protein N was not expressed when cells were pretreated with a small interfering RNA (siRNA) directed against the protein N, emphasized that progeny virus, and not input virus, was quantified in these assays (Figures 2C and 2D). Moreover, staining with anti-DC-SIGN and anti-UUKV mAbs showed that infection increased with increasing DC-SIGN expression (Figure 2E).

To confirm that the infection was mediated by DC-SIGN, we utilized inhibitors of the lectin: EDTA, mannan, and the mAb 1621. EDTA inhibits DC-SIGN by extracting the bound calcium, and mannan is a competitor of insect-derived glycans. Both inactivate DC-SIGN (Lozach et al., 2005). The increase in infectivity due to DC-SIGN expression was significantly reduced for all four viruses in cells treated by these inhibitors (Figure 2F).

Together, these results showed that phleboviruses efficiently infect human DCs, that infection is mediated by DC-SIGN, and that DC-SIGN ectopically expressed in cell lines supports infection. Although infection with UUKV did not result in efficient virus production in human DCs, the virus could be used to investigate the entry of bunyaviruses and the role of DC-SIGN. In all further experiments, we used UUKV because it is safe to work with and its utilization allows approaches such as live cell imaging nearly impossible for pathogenic bunyaviruses, most of which must be handled in high biosafety laboratories.

DC-SIGN Enhances Binding of UUKV to Cells

To determine whether DC-SIGN enhanced infection by promoting bunyavirus binding, we utilized fluorescently labeled UUKV particles (Lozach et al., 2010). These could be visualized as single spots by confocal microscopy; no significant impact of labeling on infectivity was observed (data not shown). When Alexa Fluor 594- and Bodipy Texas Red-conjugated UUKV (UUKV-AF594 and UUKV-TR) were used in combination with confocal microscopy or FACS, binding to DC-SIGN-expressing HeLa and Raji cells could be quantified at a moi of 0.04 and higher (Figures 3A and 3B). Binding increased with increasing concentration of input UUKV-TR under conditions in which no binding was observed to parental cells (Figure 3C). The presence of the DC-SIGN inhibitors described above blocked virus binding on Raji-DC-SIGN cells and DCs (Figures 3D to 3F). These experiments indicated that DC-SIGN supported UUKV binding and that the interaction was specific.

High-Mannose *N*-Glycans Are Responsible for UUKV Binding to DC-SIGN

Like other bunyaviruses, UUKV has several *N*-linked oligosaccharides in its envelope glycoproteins G_N and G_C (four sites each). To determine whether they mediate binding to DC-SIGN, we analyzed the glycosylation pattern. UUKV produced in mammalian cells (BHK-21) was treated with endoglycosidase H (Endo H) and peptide:*N*-glycosidase F (PNGase F) before SDS-PAGE and western blotting (Figure 3G). Under reducing conditions, both glycoproteins were sensitive to Endo H, with only one *N*-glycosylation site remaining resistant. These results demonstrated that UUKV, even when produced in mammalian cells, has mainly high-mannose *N*-glycans.

To evaluate the role of glycans in virus attachment, we subjected intact viruses to PNGase F and Endo H. The enzyme treatment did not significantly affect UUKV infectivity, and deglycosylated particles were not aggregated when observed by electron microscopy (EM) (Figure 3H). Regardless of which of the enzymes was used, the capacity of the viruses to bind to cells expressing the lectin was significantly reduced (Figure 3I). That binding was not completely inhibited after pretreatment with PNGase F was probably due to inefficient digestion under nondenaturing conditions. Altogether, the results show that high-mannose *N*-glycans in G_N and G_C play a central role in UUKV binding to DC-SIGN-expressing cells.

DC-SIGN Binds UUKV through Direct Interactions

When DCs and HeLa-DC-SIGN cells with bound viruses were subjected to thin-section EM, viral particles could be observed on the entire cell surface (Figure 4A). Some were seen within clathrin-coated pits (CCPs), others in shallow plasma membrane (PM) indentations without a visible cytoplasmic coat (white and black arrowheads respectively). The distances between the surface of the virus and the PM of DCs and HeLa-DC-SIGN cells were 22.6 ± 6.0 nm (n = 46) and 22.0 ± 8.1 nm (n = 42), respectively, consistent with the length of DC-SIGN ectodomain (20–30 nm) (Feinberg et al., 2005; Menon et al., 2009). In marked contrast, parental HeLa cells were seen to bind much fewer particles, and the distance between viruses and cell membrane was 10.2 ± 3.8 nm (n = 8) (data not shown).

Confocal microscopy after immunostaining with anti-DC-SIGN mAbs showed that the bound UUKV-AF594 particles were associated with DC-SIGN-containing spots and areas (Figure 4B). To better visualize a possible interaction, we used live cells and total internal reflection fluorescence microscope (TIRFM). The cytosolic tail of the lectin was fluorescently tagged with a monomeric version of enhanced green fluorescent protein (mEGFP) (Figure 4C). HeLa cells were transduced with the HR-SEW lentiviral vector encoding the fusion protein (mEGFP-DC-SIGN) and sorted for high expressors. The protein had the expected molecular weight (~70 kDa) (Figure 4D). The fraction of the tagged lectin present on the cell surface was sufficient to support UUKV infection (Figures 4E–4G). Moreover, mAbs neutralizing DC-SIGN blocked infection (Figure 4G).

(E) UUKV-AF594 (moi ~0.5) was bound to DCs on ice in the presence of the anti-DC-SIGN mAb 1621 (50 $\mu g \cdot ml^{-1}$) and imaged by confocal microscopy. Spots are cell-associated particles seen in a series of z stacks merged to one plane. Nuclei were stained with DRAQ5.
(F) Bound particles per DC in the absence (n = 37) and presence (n = 45) of the anti-DC-SIGN mAb 1621 were counted in ten independent fields from (E).
(G) UUKV (250 ng viral glycoproteins) was digested with PNGase F or Endo H (2000 units) under reducing conditions for 4 hr at 37°C. Samples were analyzed by western blotting with polyclonal Abs against UUKV glycoproteins G_N and G_C.
(H) UUKV-TR (250 ng viral glycoproteins) was treated with PNGase F or Endo H (1500 units) under nondenaturing conditions for 1 hr at 37°C and assessed for infectivity by plaque assay. The particles were also negatively stained and viewed by EM. The scale bar represents 100 nm.
(I) UUKV-TR (20 nM viral glycoproteins) was bound to Raji-DC-SIGN cells on ice after treatment with PNGase F or Endo H as described in (H). Binding was analyzed by FACS and normalized to binding of untreated UUKV-TR (No enzyme) to Raji-DC-SIGN cells. Error bars represent the SD.

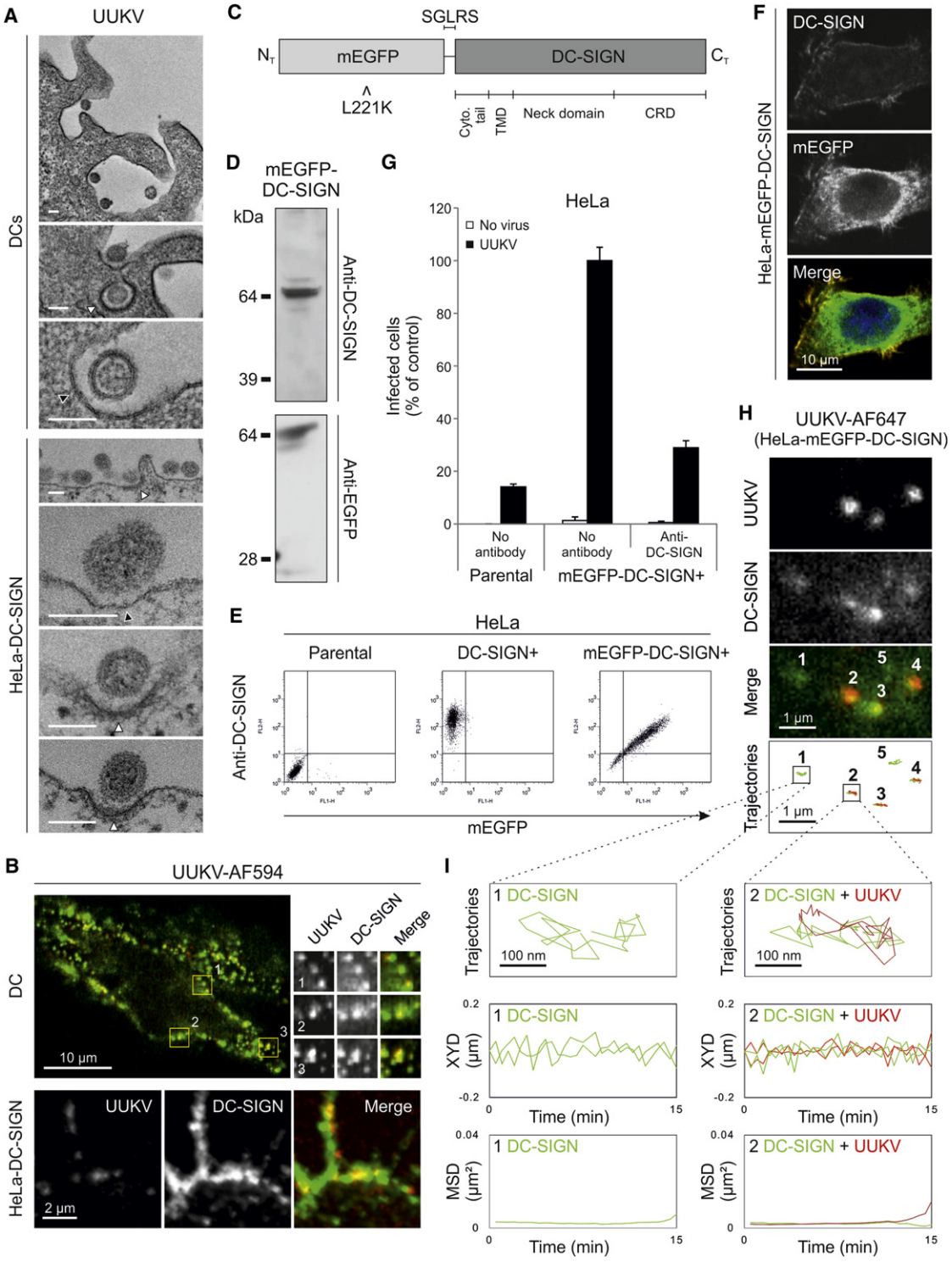

Figure 4. UUKV Binds to DC-SIGN through Direct Interactions

(A) UUKV (moi ~100) was bound to DCs and HeLa-DC-SIGN cells on ice before fixation and analyzed by thin-section EM. Some of the membrane-bound viruses were associated with invaginations (black arrowheads) and CCPs (white arrowheads) at the PM. Scale bars represent 100 nm.

(B) UUKV-AF594 was bound to DCs and HeLa-DC-SIGN cells (moi ~1) on ice. Cells were fixed, permeabilized, and stained with an anti-DC-SIGN mAb before imaging by confocal microscopy. UUKV (red) and DC-SIGN (green) are shown in one focal plane. Magnifications of association between UUKV and DC-SIGN on DCs (yellow squares) are shown on the right.

(C) The cytosolic tail (Cyto. tail) of DC-SIGN was tagged with mEGFP by inserting the cDNA sequence coding for DC-SIGN into the expression vector pmEGFP-C1. mEGFP is a monomeric version of EGFP with the dimer interface destroyed by the L221K mutation. TMD, transmembrane domain.

Thus, the results indicated that mEGFP-tagged DC-SIGN mimicked the function of the wild-type (WT) molecule.

For visualization cell-bound particles by TIRFM, the viruses have to be localized between the cell and the coverslip. Small viruses such as murine polyoma virus can diffuse into this narrow space (Ewers et al., 2005), but larger viruses such as UUKV do not. We used two methods to localize the virus between the cell and the coverslip. In the first case, mEGFP-DC-SIGN-expressing cells were detached from the culture plate with EDTA, exposed to AF647-conjugated UUKV (UUKV-AF647) in suspension on ice, and seeded on coverslips. The second procedure involved prebinding of viruses to coverslips coated with extracellular matrix (ECM) as previously described (Johannsdottir et al., 2009) and seeding of cells on top of the bound viruses. One technical problem was that it takes ~5 min to set up the TIRFM and start recording, which means that reactions are already well on their way before recording starts. To slow down the process, the cells were subjected to imaging by dual-color TIRFM at room temperature.

With the first protocol, UUKV could be seen to colocalize with clusters of mEGFP-DC-SIGN (Figure 4H). The overall distribution of lectin staining was uneven with clusters present without any virus association, consistent with previous reports on DC-SIGN clustering on the cell surface (de Bakker et al., 2007; Neumann et al., 2008). To analyze the dynamics of the virus and the receptor clusters, we recorded and analyzed 25 particles and DC-SIGN-enriched domains over time from nine cells. We determined trajectories from digital images by linking positions from frame to frame using a single-particle tracking algorithm (Sbalzarini and Koumoutsakos, 2005). Representative trajectories are shown in Movie S1 and Figures 4H and 4I, with the corresponding XY and mean-square (MSD) displacements. Whether initially bound to coverslips (data not shown) or cells, the viruses were virtually immobile. Similar results were obtained when viruses were bound to cells expressing untagged DC-SIGN (data not shown).

UUKV Binding to DC-SIGN Induces Receptor Clustering

To determine whether the viruses bound to preformed clusters or recruited receptors to the site of binding, we followed ECM-bound virus particles over time after contact with cells. In this case, the particles were attached to the matrix and could not undergo endocytosis. Under these conditions, we could record the fluorescence of 22 UUKV particles in 12 cells with associated mEGFP-DC-SIGN receptor. The Image J-based plugin Particle-Tracker (Sbalzarini and Koumoutsakos, 2005) was used to quantify the fluorescence intensities. In seven of these recordings, the relative ratio between virus and receptor fluorescence did not change over a period of 15 min (Figure 5A, High). In nine cases, there was a slight increase (about 2-fold). However, in six cases the receptor fluorescence was initially weak, but increased strongly (3- to 4-fold) within the first 3–5 min. Examples of this are shown in Movie S2, Figure 5A (Low), and Figure 5B. In these cases the number of receptors associated with the virus increased over time to reach a plateau value within 3–5 min. At 37°C, the process is likely to be faster.

UUKV Is Efficiently Internalized in DC-SIGN-Expressing Cells

To test whether DC-SIGN facilitates UUKV endocytosis, we exposed HeLa-DC-SIGN cells to AF488-conjugated particles (UUKV-AF488) at 4°C, washed them to remove unbound material, and rapidly warmed them to allow internalization. To distinguish between internalized and surface-bound particles, we used an assay based on treatment with trypan blue as recently described (Engel et al., 2011). Trypan Blue is membrane impermeable, and thus only able to quench the fluorescence of UUKV-AF488 particles still exposed on the cell surface. When the generation of trypan blue-resistant UUKV-AF488 was analyzed over time, it was found that most particles were internalized within 10–15 min (Figure 5C). Taking into account the background fluorescence, we estimated that the half-maximal level of internalization was reached within 4 min and that about 50% of the cell-bound particles were endocytosed. The kinetic of virus uptake into DCs was slightly faster (Figure 5C).

To analyze internalization using EM, we exposed cells to UUKV at high moi on ice, and rapidly shifted them to 37°C to allow endocytosis. After 3 min, viruses were seen in clathrin-coated (CCVs) and smooth-surfaced vesicles with a diameter of about 150–200 nm, close to the PM (Figure 5D, #1 and #2). After 10 min, UUKV was also observed in classical early endosomal (EE) vacuoles with diameters of 400–500 nm (Figure 5D, #3 and #4). Some of the EEs had electron-dense coats on their cytosolic surface (Figure 5D, #4), characteristic of protein clusters containing clathrin and the endosomal sorting complex required for transport (ESCRT).

We recently showed in human, rodent, and monkey cells that infectious entry of UUKV is pH dependent (Lozach et al., 2010). We observed that UUKV infection in DC-SIGN-expressing cells

(D–F) mEGFP-DC-SIGN-expressing HeLa (HeLa-mEGFP-DC-SIGN) cells were obtained by retroviral transduction and FACS sorting. The specificity of the fusion protein mEGFP-DC-SIGN was controlled by western blotting (D), and, at the cell surface, by FACS (E) and confocal microscopy (F). DC-SIGN (red) and mEGFP (green) are shown in one focal plane. Nuclei were stained with DRAQ5.

(G) HeLa and HeLa-mEGFP-DC-SIGN cells were infected with UUKV (moi ~10) in the presence of the anti-DC-SIGN mAb 1621 (25 $\mu g \cdot ml^{-1}$). Infection was analyzed by FACS 18 hr later and normalized to infection of HeLa-mEGFP-DC-SIGN cells in the absence of Abs (38% of cells were infected in this sample). Error bars represent the SD.

(H) Fluorescent UUKV particles (UUKV-AF647, moi ~0.5) were bound to HeLa-mEGFP-DC-SIGN cells on ice. Cells were then seeded on coverslips before warming to room temperature. mEGFP-DC-SIGN (green) and UUKV-AF647 (pseudocolored red) were imaged by TIRFM on the bottom cell surface. DC-SIGN and UUKV trajectories (green and red, respectively) were recorded at 1/30 Hz (31 frames, lower panel). Numbers 1 and 5 show DC-SIGN motion alone, and 2 to 4 show coordinated motions with UUKV.

(I) Magnifications of trajectories 1 and 2 obtained in (H). Below each are the respective analytical plots: absolute XY (XYD) and mean-square (MSD) displacements versus time.

See also Movie S1.

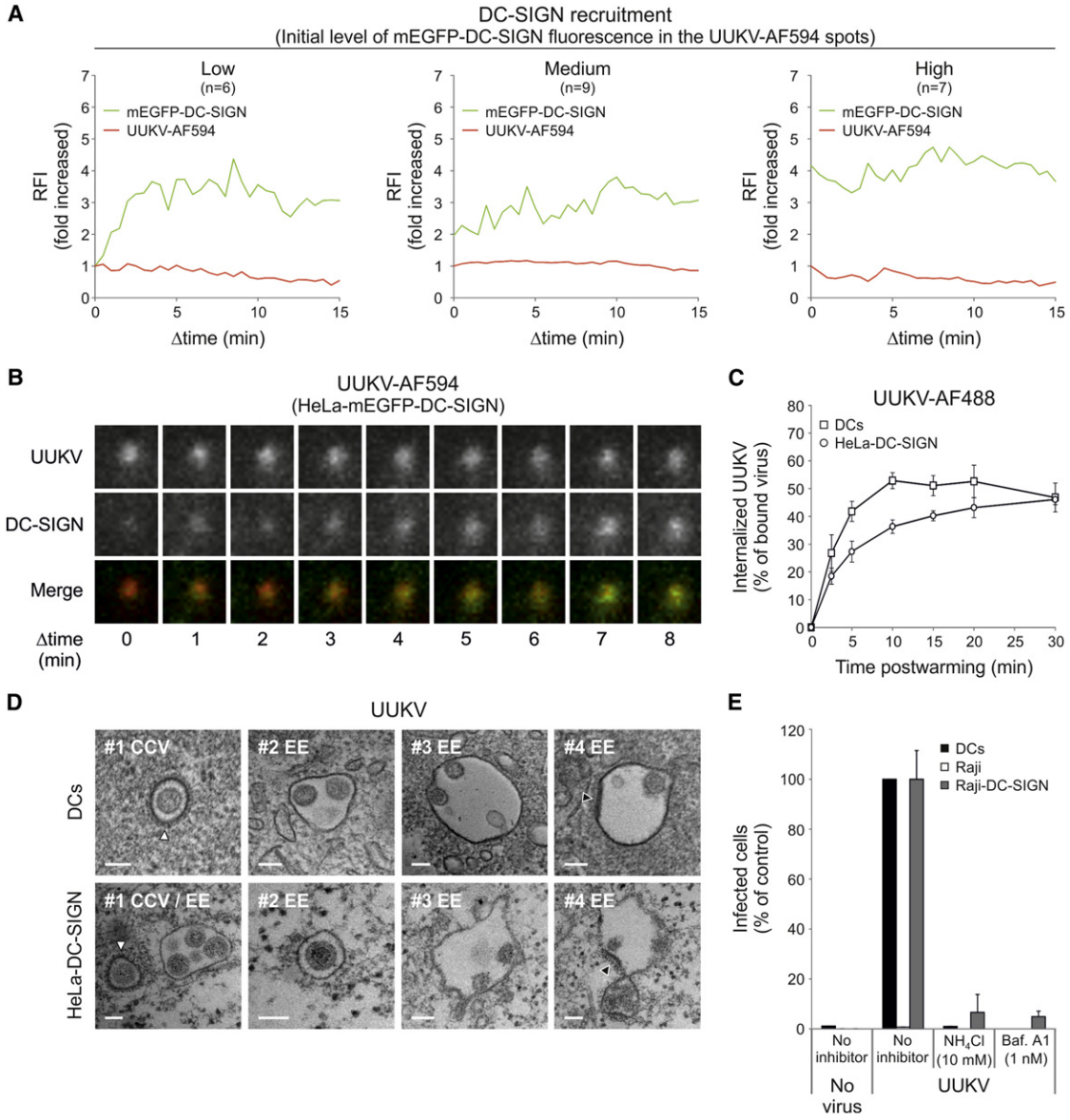

Figure 5. UUKV Induces DC-SIGN Clustering before Internalization

(A) UUKV-AF594 (moi ~0.5) was immobilized to ECM on ice before addition of HeLa-mEGFP-DC-SIGN cells. Live-cell imaging was performed on bottom cell surface by TIRFM at room temperature for 15 min. DC-SIGN recruitment was analyzed for UUKV-AF594 spots associated with different initial densities of lectin (named low, medium, and high). A representative trend of fluorescence variation is shown for each. Values are given as fold increase over time zero of the left panel.

(B) Time-lapse series of DC-SIGN recruitment (green) by a confined viral particle (red) when initial lectin density is low.

(C) Fluorescent UUKV particles (UUKV-AF488, moi ~1) were bound to DCs and HeLa-DC-SIGN cells on ice before warming to 37°C for up to 30 min. Internalization was analyzed by FACS after cell fixation and trypan blue treatment to quench fluorescence due to cell-surface bound viruses. Internalization is given as the percentage of fluorescence measured in samples not treated with trypan blue (percent of bound virus). The fluorescence observed for cells not exposed to UUKV-AF488 was considered as background and subtracted from other values. Error bars represent the SD.

(D) UUKV (moi ~100) was bound to DCs and HeLa-DC-SIGN cells on ice. Cells were then rapidly warmed for 10 min before fixation and analysis by thin-section EM. Viruses were seen in CCVs (#1, white arrowhead) and in small, uncoated vesicles (#2). UUKV was also observed in larger endosomal structures (#3 and #4). Black arrowheads indicate ESCRT structures. The scale bar represents 100 nm.

(E) DCs and Raji-DC-SIGN cells were infected with UUKV (moi ~1) in the presence of pH interfering drugs. Infection was quantified by FACS 8 hr later and normalized to infection in the absence of inhibitors. Baf A1 for bafilomycin A1. Error bars represent the SD.

See also Movie S2.

was also sensitive to agents that neutralize vacuolar pH such as ammonium chloride (NH_4Cl), a lysomotropic weak base, and bafilomycin A1, a vacuolar-type H^+-ATPase inhibitor (Figure 5E). Altogether, the results show that UUKV entry into DC-SIGN-expressing cells involves endocytic internalization, acidification, and at least in part, CCPs and CCVs.

DC-SIGN by Itself Promotes UUKV Internalization

The DC-SIGN cytosolic tail carries several sequence motifs (a dileucine, LL, a tyrosine-based, YXXΦ, and a triacidic motif, EEE) believed to serve as signals for endocytic internalization, intracellular trafficking, and signaling (Svajger et al., 2010). The classical LL motif present in the lectin cytosolic tail has been shown to be critical for DC-SIGN endocytosis (Engering et al., 2002; Sol-Foulon et al., 2002). To investigate the role of this motif in UUKV internalization, we generated HeLa and Raji cells stably expressing a DC-SIGN mutant devoid of the LL sequence (DC-SIGN LL) (Lozach et al., 2005). Regardless of the line, the mutant was slightly higher expressed than the WT lectin (DC-SIGN WT) (data not shown). We found that DC-SIGN LL bound UUKV with the same efficiency as cells expressing DC-SIGN WT (Figure 6A), consistent with a previous report (Lozach et al., 2005).

To determine whether they internalized the virus, we incubated DC-SIGN LL-expressing cells with UUKV-AF594 in the cold and rapidly warmed them to 37°C to allow internalization. Although warming induced a dramatic redistribution of UUKV-AF594 in DC-SIGN WT-expressing HeLa cells, consistent with intracellular accumulation of viral particles, DC-SIGN LL-bound UUKV-AF594 remained mainly at the cell surface (Figure 6A). Spinning-disc confocal videomicroscopy of live cells also showed that octadecyl rhodamine B chloride-conjugated UUKV (UUKV-R18) was taken up by HeLa-DC-SIGN WT cells but not by cells expressing DC-SIGN LL (Movie S3 and Movie S4). Live cell imaging with TIRFM confirmed that UUKV-AF488 accumulated only in subcellular compartments of HeLa-DC-SIGN WT cells (Figure 6B, Movie S5, and Movie S6). That fluorescence was not quenched after trypan blue treatment demonstrates that the particles had been internalized.

DC-SIGN-Mediated Endocytosis of UUKV Is Critical for Infection

We then assessed whether loss of the LL motif impaired UUKV infection. We found that Raji and HeLa cells expressing DC-SIGN LL were less efficiently infected than DC-SIGN WT-expressing cells, with even higher differences at lower moi (Figure 6C, right panel, and Figure 6D). Bypassing the need for endocytosis during productive infection as recently described (Lozach et al., 2010), i.e., fusing viruses at the PM, resulted in efficient infection of parental Raji cells at moi ~10 (Figure 6C, pH ~5.0). At such a moi, the parental cells could not be infected under normal conditions (Figure 6C, $-NH_4Cl$). This strongly supported the notion that the few viruses that bound to parental cells at high moi could not undergo endocytosis. That levels of replication in bypass experiments were similar in DC-SIGN WT- and DC-SIGN LL-expressing cells, regardless of the moi, indicated that cells expressing the mutant could be infected.

To compare the timing of the acid-requiring step after endocytic entry into DC-SIGN WT- and DC-SIGN LL-expressing HeLa cells, we bound virus to cells on ice and rapidly shifted the temperature to 37°C to allow endocytosis. NH_4Cl was added at different times after warming to prevent further virus penetration. The entry process was significantly faster in cells expressing DC-SIGN WT, including DCs (Figure 6E). Infectious penetration started after 3–5 min lag and reached a half-maximal level within 9–15 min. Taken together, these results show that the endocytosis-defective mutant of the lectin was unable to mediate UUKV uptake and infection. Therefore, DC-SIGN does not merely serve as an attachment factor but also as a true receptor required for endocytosis.

Virus Dissociates from DC-SIGN after Internalization

To monitor UUKV and DC-SIGN trafficking after internalization, we exposed HeLa-DC-SIGN cells to UUKV-AF594 on ice and rapidly them shifted to 37°C for up to 30 min to allow endocytosis. Cells were fixed, permeabilized, immunostained with anti-DC-SIGN mAbs, and analyzed by confocal microscopy. Five minutes after warming, all internalized particles were associated with cytoplasmic DC-SIGN-positive vesicles (Figure 7A). This indicated that the virus was internalized together with the receptor. However, thereafter the amount of internalized viruses colocalizing with DC-SIGN decreased until no longer detectable after 20 min (Figure 7A). At this time, viruses accumulated in the perinuclear region and after 30 min they were all associated with vacuoles containing the LE and lysosome marker LAMP1 (EGFP-LAMP1) (Figure 7B). The kinetic of colocalization with the lectin in DCs was rather similar (Figure 7C). These data showed that, after capture and internalization, the viruses dissociated from DC-SIGN in EEs and continued in the degradative pathway to LEs and lysosomes.

DISCUSSION

As an abundant immune receptor on dermal DCs, DC-SIGN is thought to be critical for the capture of incoming pathogens by their surface glycans, thus promoting antigen processing and subsequent presentation (Svajger et al., 2010; van Kooyk, 2008). The acquired immune response is thus initiated. It has been proposed that some viral pathogens (including human immunodeficiency virus and arboviruses of the flavi- and alphavirus families) have found a way to use DC-SIGN for attachment and to promote entry and infection (Svajger et al., 2010).

In this study, we have expanded these observations to bunyaviruses. We found that several phleboviruses including PTV, RVFV, TOSV, and UUKV use DC-SIGN to infect immature DCs and cells expressing the lectin ectopically. We also found that DC-SIGN promoted infection by Germiston virus, an orthobunyavirus (data not shown). Others have shown that hanta- and nairoviruses have glycoproteins with high-mannose *N*-glycans (Sanchez et al., 2002; Schmaljohn et al., 1986) and that immature DCs support their infection (Connolly-Andersen et al., 2009; Raftery et al., 2002). Although the interaction of additional bunyaviruses with DC-SIGN must be assessed experimentally, it is likely that many can use DC-SIGN as a receptor.

One of the phleboviruses, UUKV, was used to further analyze the role of the lectin in the infection process. Closely related to RVFV, this tick-borne virus can infect human cells, but progeny virus production is minimal. While the type of glycans synthetized in tick cells is poorly characterized, UUKV glycoproteins G_N and G_C were found to carry mainly high-mannose glycans after synthesis in rodent cells. The reason that the glycans fail to undergo efficient terminal glycosylation in mammalian cells may be that UUKV like other bunyaviruses buds into the ERGIC or the *cis*-most stacks of the Golgi (Kuismanen et al., 1982). The glycoproteins may escape full exposure to glycosidases and

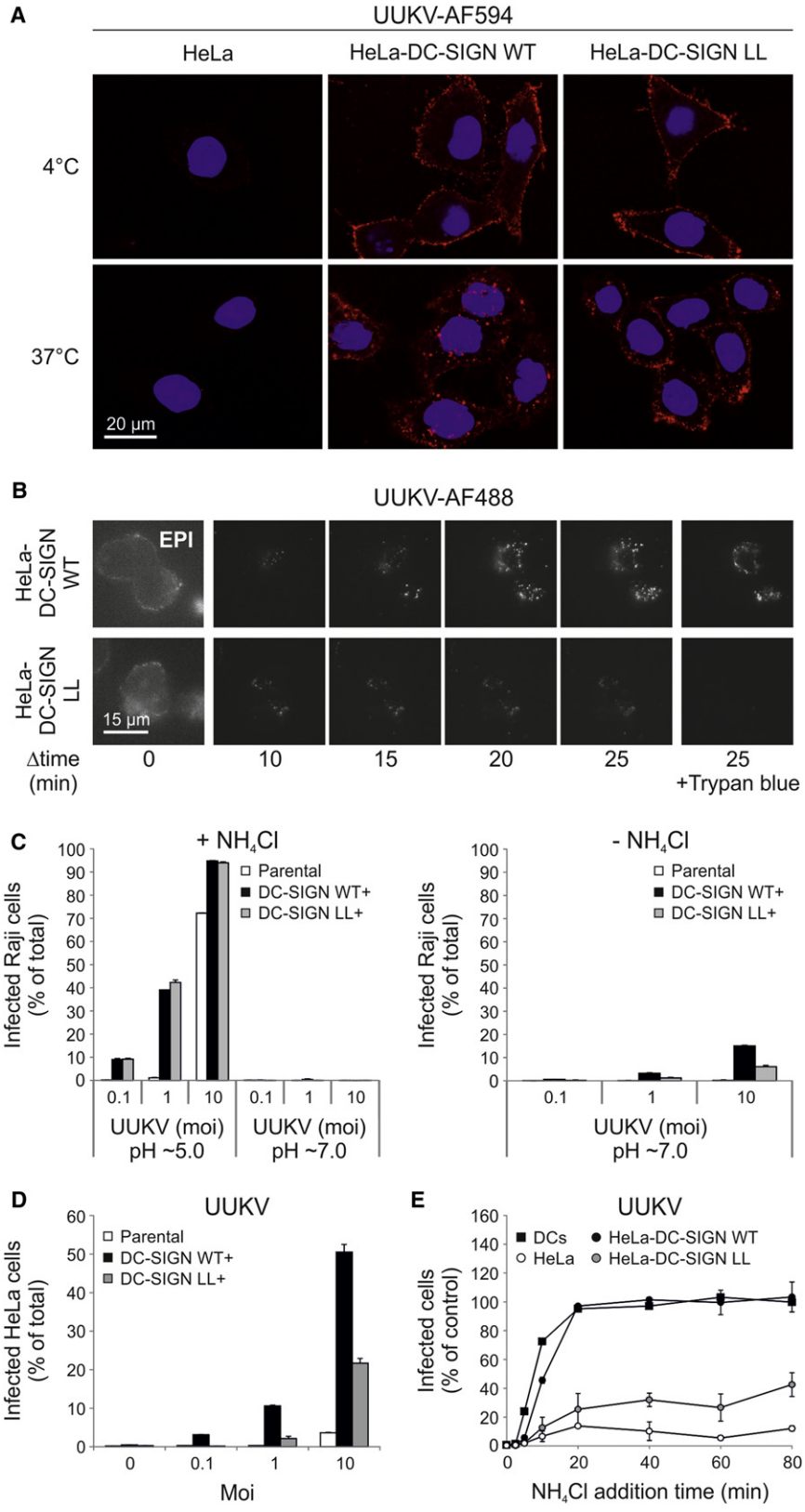

Figure 6. DC-SIGN Endocytic Activity Is Critical for UUKV Uptake

(A) UUKV-AF594 (moi ~5) was bound to HeLa cells expressing DC-SIGN WT (HeLa-DC-SIGN WT) or the DC-SIGN endocytosis-defective mutant (HeLa-DC-SIGN LL). Cells were maintained on ice or warmed for 30 min before fixation and imaging by confocal microscopy. Red spots are cell-associated virus particles seen in one focal plane. Nuclei were stained with DRAQ5.

(B) UUKV-AF488 (moi ~1) was bound to HeLa-DC-SIGN WT and HeLa-DC-SIGN LL cells on ice before allowing cells to attach on coverslips. The cytoplasm was illuminating with TIRFM (1/30 Hz) at 37°C for 25 min. Initial amounts of bound particles are shown by epifluorescence (EPI) microscopy. Internalization was confirmed by addition of trypan blue at the end of analysis.

(C) DC-SIGN WT- and DC-SIGN LL-expressing Raji cells were exposed to UUKV on ice, washed, and treated at the indicated pHs at 37°C for 1.5 min. Infected cells were incubated for 16 hr at 37°C in the presence of NH_4Cl (50 mM) to block penetration from endosomes and analyzed by FACS. Note that Raji cells had here lower DC-SIGN WT expression than in the previous experiments (data not shown). Error bars represent the SD.

(D) HeLa-DC-SIGN WT and HeLa-DC-SIGN LL cells were infected with UUKV before FACS analysis 8 hr later. Error bars represent the SD.

(E) DCs, HeLa-DC-SIGN WT and HeLa-DC-SIGN LL cells were exposed to UUKV (moi ~5) on ice, washed, and rapidly warmed. NH_4Cl (50 mM) was added at different times to block further penetration. Infection was detected by FACS 18 hr later and normalized to infection in the absence of NH_4Cl. Error bars represent the SD.

See also Movie S3, Movie S4, Movie S5, and Movie S6.

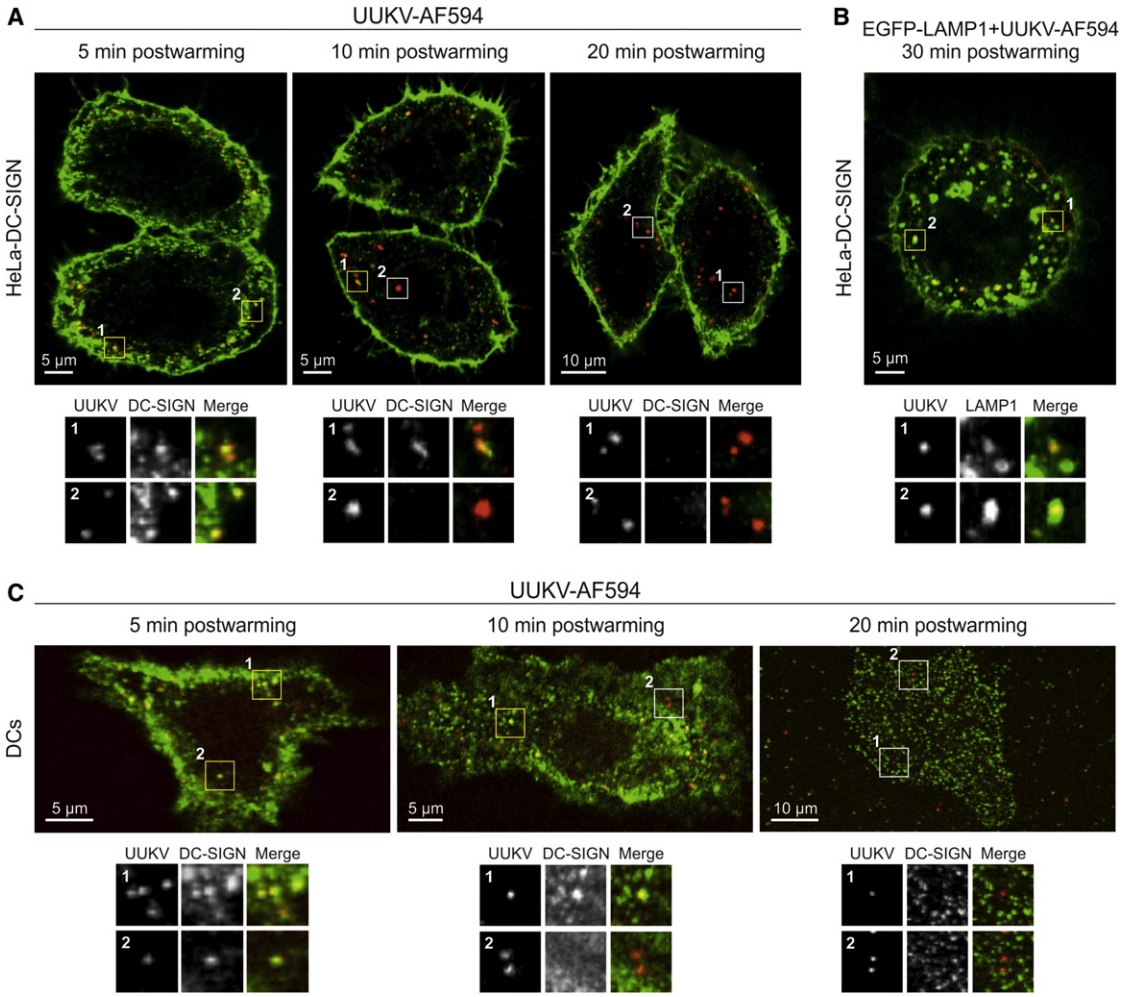

Figure 7. UUKV Dissociates from DC-SIGN after Internalization

UUKV-AF594 (moi ~1) was bound to HeLa-DC-SIGN (A), EGFP-LAMP1-expressing HeLa-DC-SIGN cells (B), and DCs (C) on ice. Cells were washed, rapidly warmed for up to 30 min, and fixed. UUKV (red) and DC-SIGN (A and C) or EGFP-LAMP1 (B) (green) were imaged in one focal plane by confocal microscopy. DC-SIGN was detected by immunostaining after cell permeabilization. Magnifications of association between UUKV and green vesicles (yellow squares) or noncolocalizing, internalized particles (white squares) are shown on the bottom.

glycosyltransferases because they move through the Golgi as part of a virus particle and not as integral membrane proteins like most other viral glycoproteins. Alternatively, these viruses may escape *N*-glycan modifications by exiting cells from the first stacks of the Golgi.

Like other arboviruses, bunyaviruses produced in insect vectors have exclusively high-mannose glycans in their envelope glycoproteins. After transmission via insect bites, they are likely to be specifically recognized by DC-SIGN on DCs in the dermis. It is conceivable that these viruses have evolved a common strategy shared with unrelated arboviruses such as flaviviruses to subvert DC-SIGN to initiate host infection. However, that bunyaviruses are rich in high-mannose glycans even produced in mammalian cells suggests that they do not require production in insects to be recognized by DC-SIGN. It is unlikely that viral progeny coming from dermal DCs follow a similar strategy after spread into the host. DC-SIGN expression is restricted to dermal DCs, and while the immature DCs express high levels of DC-SIGN, maturation of DCs leads to downregulation of the lectin (van Kooyk, 2008). Activation of immature DCs by bunyaviruses has been reported (Peyrefitte et al., 2010; Raftery et al., 2002). Progeny virus coming from DCs could use other C-type lectins with high affinity for mannose residues to target and infect new tissues in hosts, e.g., L-SIGN or LSECtin.

In DC-SIGN-expressing cells, the lectin was distributed over the PM in clusters of different sizes. Most of the bound UUKV particles were associated with these. The bound viruses underwent random lateral motion, but the distances traveled were small. When individual fluorescent viruses were visualized at room temperature by TIRFM in cells expressing mEGFP-tagged DC-SIGN, it was often possible to observe a process of mEGFP-DC-SIGN recruitment to bound virus particles. At room temperature, the virus-associated DC-SIGN fluorescence increased as much as 3- to 4-fold over a period of 3–5 min. At 37°C, the rate of receptor recruitment was likely to be faster. In general, the observations were consistent with theoretical

simulations of virus binding to mobile cellular receptors (English and Hammer, 2005). Attachment to the cell surface is most probably initiated by a few contacts, and then tightened as more DC-SIGNs are recruited to the virus surface.

Our video recordings allow the visualization of receptor recruitment to cell-associated virus particles. They confirm the hypothesis that viruses collect receptors to the site of contact and thus generate a receptor-rich microdomain in the PM. The lipid and protein composition, the curvature, the association with the actin cortex, and other properties may differ in these virus-induced membrane patches from the membrane at large, and this may significantly influence the next events including signal transduction and endocytosis.

Using Abs, it has been shown that crosslinking on the cell surface is required to induce efficient endocytosis of DC-SIGN in DCs (Neumann et al., 2008). Hence, the most likely scenario is that UUKV-induced clustering of DC-SIGN leads to the activation of a signaling pathway that triggers endocytic uptake of the receptor cluster and the ligand. DC-SIGN has been recently reported to be involved in different signaling pathways (Svajger et al., 2010). DC-SIGN was internalized together with the incoming viral particles. When a mutant DC-SIGN was expressed lacking the LL motif in the cytosolic tail, the viruses still attached to the cells, but they were not internalized and there was no infection. This confirmed that DC-SIGN served as a true receptor, not only as an attachment factor.

Our results contrast with a previous report on the unrelated dengue (DV) arbovirus, for which it was proposed that the internalization is independent of the DC-SIGN endocytosis signals (Lozach et al., 2005). This virus may use the lectin in a different way; several mechanisms have been described for interactions between DC-SIGN and pathogens (Svajger et al., 2010). However, we cannot exclude that DC-SIGN by itself also mediates DV internalization. The investigation with DV was based on the detection of viral replication up to 48 hr after infection, whereas UUKV allowed an accurate analysis of virus uptake within a few minutes after internalization.

EM showed that many of UUKV particles on the cell surface were in CCPs, and after warming, viruses could be observed in coated vesicles. Although our results are not conclusive, a growing body of evidence favors the clathrin-mediated endocytosis (CME) route as the main pathway of DC-SIGN-mediated entry. First, DC-SIGN-mediated uptake of soluble antigens is impaired in the presence of clathrin inhibitors (Cambi et al., 2009). Second, it has been shown that LL-based motifs, like those in the cytosolic tail of DC-SIGN, are involved in the uptake of various cargo into CCVs (Bonifacino and Traub, 2003).

Once the UUKV particles reached endosomes, our results indicated that the viruses separated from DC-SIGN. Separation occurred 5–10 min after internalization, at a time when DC-SIGN shares the compartment with transferrin (Sol-Foulon et al., 2002). This was consistent with reports that DC-SIGN tetramers undergo acid-induced disassembly below pH 6.5–6.7 and thereby lose their high avidity for cargo (Guo et al., 2004; Tabarani et al., 2009). Apparently, DC-SIGN belongs to the receptors that recycle from EEs to the PM leaving cargo behind (Engering et al., 2002). Like other late penetrating viruses (Lozach et al., 2010), UUKV continues its journey into the degradative pathway.

The general properties and dynamics of UUKV entry into DCs were very similar to the ones observed in cell lines expressing DC-SIGN, often even slightly faster and more efficient. This emphasizes the strength of the findings in this study, which could not be assessed in DCs, i.e., receptor clustering and DC-SIGN-mediated internalization. To perform such investigations in DCs, endogenous DC-SIGN expression had to be silenced by siRNAs before transfection with plasmids encoding the mEGFP-tagged lectin or DC-SIGN LL. When this was attempted, the analysis was not possible because of low transfection efficiency and cell viability.

Although it remains to be confirmed under physiological conditions, we propose that by acting as an endocytic receptor in dermal DCs, DC-SIGN plays a critical role in the initial transmission after bites by arthropods infected with bunyaviruses. In further rounds of infection, it is apparent that these viruses use other cell types and receptors. Bunyaviruses can infect a wide spectrum of tissues, most of which do not express DC-SIGN (Schmaljohn and Nichol, 2007; Svajger et al., 2010). We have analyzed the interaction of UUKV with cells devoid of DC-SIGN, and found that the general properties of the entry process are similar to those described here but much less efficient (Lozach et al., 2010). The identity of the receptors involved remains unknown.

EXPERIMENTAL PROCEDURES

Cells and Viruses

Cell lines expressing DC-SIGN WT, DC-SIGN LL, and mEGFP-DC-SIGN were generated by transduction with the TRIPΔU3 and HR-SEW lentiviral vectors as previously reported (Lozach et al., 2005). DCs were obtained by differentiation of isolated human PBMCs using a standard procedure (Lozach et al., 2005). The prototype strains of PTV, RVFV ZH548, TOSV ISS, and UUKV S23 have been described previously (Giorgi et al., 1991; Laughlin et al., 1979; Pettersson and Kääriäinen, 1973). Production, purification and titration of viruses were performed in the mammalian Vero and BHK-21 cells as shown elsewhere (Billecocq et al., 1996; Lozach et al., 2010). Labeling of UUKV with AF-succinimidyl esters and Bodipy TR-thiosulfates (Invitrogen) was performed in HEPES (20 mM) as recently described (Lozach et al., 2010). Alternatively, UUKV (10^9 ffu ml^{-1}) was labeled with the lipid dye R18 (20 μM, Invitrogen) according to a similar protocol. The moi is given according to the titers determined on BHK-21 and Vero cells.

Virus Deglycosylation

Viruses (250 ng glycoproteins) were subjected to Endo H and PNGase F (2000 units, New England Biolabs) as previously shown (Lozach et al., 2005). Native deglycosylated viruses could be obtained when samples were incubated with each enzyme (1500 units) for 1 hr at 37°C, with the denaturing step and the Nonidet P-40 buffer (New England Biolabs) omitted.

Binding Assay

Viruses were bound to the cells for 1 hr on ice at various moi in binding buffer (RPMI pH ~7.4 containing 0.2% BSA, 1 mM $CaCl_2$, and 2 mM $MgCl_2$) as described before (Lozach et al., 2010). Binding was quantified by FACS or analyzed by fluorescence microscopy. When used for microscopy, DCs were stretched on fibronectin-coated coverslips for 1 hr at 37°C. For binding inhibition, cells were pretreated with inhibitors for 30 min and then exposed to viruses in their presence. For EGFP-LAMP1 colocalization experiments, cells were washed 6 hr after transfection and exposed to viruses 12 hr later. For TIRFM, cells were exposed to viruses on ice and subsequently added on coverslips. Alternatively, cells were grown to confluence on coverslips. On the day of imaging, cells were removed with 2.5 mM EDTA to preserve the ECM. Viruses were bound to coated coverslips on ice before cells were allowed to attach.

Internalization Assay

Virus-bound cells were rapidly warmed to 37°C for up to 30 min. For FACS analysis, to distinguish between internalized and external particles, samples were treated with trypan blue (0.01%, Sigma) for 15 s at room temperature (Engel et al., 2011).

FACS-Based Infection and PM-Virus Fusion Assays

Cells were infected as previously shown (Lozach et al., 2010). After fixation and permeabilization with 0.05% saponin, infection was detected by standard immunostaining and quantified by FACS analysis. For inhibition assays, cells were pretreated with inhibitors for 30 min and exposed to viruses in their presence. Protein silencing was achieved by transfecting cells once with siRNA as previously described (Lozach et al., 2010). NH_4Cl add-in time course and PM-virus fusion assay were performed as recently reported (Lozach et al., 2010).

Fluorescence Microscopy

For confocal microscopy, cells exposed to fluorescent particles were analyzed with Zeiss LSM510 Meta and spinning-disc Visitech microscopes. Nuclei were stained with DRAQ5 (2.5 μM, Biostatus) when indicated. Live-cell imaging with the spinning-disc microscope was performed in the continuous presence of viruses. For monitoring of virus binding and internalization, a Leica AM TIRFM was used to illuminate bottom surface or cytoplasm of live cells by adjusting the penetration depth at 90 and 200 nm, respectively. Trajectories and fluorescence intensity of DC-SIGN and UUKV spots were analyzed by computational analysis with Image J-based plugin software (Sbalzarini and Koumoutsakos, 2005). MSD was calculated as shown elsewhere (Ewers et al., 2005).

EM

Negative staining of deglycosylated UUKV particles was performed with phosphotungstic acid at pH ~7.4 as previously described (Lozach et al., 2010). For thin-section EM, after exposure to virus (moi ~100), cells were fixed and treated as previously described (Johannsdottir et al., 2009).

Statistical Analysis

The data are representative of at least three independent experiments, except for DC-based assays, which were performed with seven healthy blood donors. Values are given as the mean of triplicates ± SD.

SUPPLEMENTAL INFORMATION

Supplemental Information includes Supplemental Experimental Procedures and six movies and can be found with this article online at doi:10.1016/j.chom.2011.06.007.

ACKNOWLEDGMENTS

This work was supported by the Swiss National Foundation, an European Research Council advanced investigator grant, the ETH Zürich, LipidX Tx, and a Marie Curie Intra European Fellowship to P.Y.L. within the 7th European Community Framework Programme. We thank F. Arenzana-Seisdedos and A. Oxenius for support, and L. Burleigh, J. Mercer, and O. Schwartz for critical reading of the paper. We also thank D. Coudrier, L. Laurent, C. Tamietti, F. Schmidt, G. Bantug, S. Bastidas, and the Flow Cytometry Laboratory of the ETH Zürich for their technical assistance.

Received: January 14, 2011
Revised: May 13, 2011
Accepted: June 15, 2011
Published: July 20, 2011

REFERENCES

Billecocq, A., Vialat, P., and Bouloy, M. (1996). Persistent infection of mammalian cells by Rift Valley fever virus. J. Gen. Virol. *77*, 3053–3062.

Bonifacino, J.S., and Traub, L.M. (2003). Signals for sorting of transmembrane proteins to endosomes and lysosomes. Annu. Rev. Biochem. *72*, 395–447.

Cambi, A., Beeren, I., Joosten, B., Fransen, J.A., and Figdor, C.G. (2009). The C-type lectin DC-SIGN internalizes soluble antigens and HIV-1 virions via a clathrin-dependent mechanism. Eur. J. Immunol. *39*, 1923–1928.

Connolly-Andersen, A.M., Douagi, I., Kraus, A.A., and Mirazimi, A. (2009). Crimean Congo hemorrhagic fever virus infects human monocyte-derived dendritic cells. Virology *390*, 157–162.

de Bakker, B.I., de Lange, F., Cambi, A., Korterik, J.P., van Dijk, E.M., van Hulst, N.F., Figdor, C.G., and Garcia-Parajo, M.F. (2007). Nanoscale organization of the pathogen receptor DC-SIGN mapped by single-molecule high-resolution fluorescence microscopy. ChemPhysChem *8*, 1473–1480.

Engel, S., Heger, T., Mancini, R., Herzog, F., Kartenbeck, J., Hayer, A., and Helenius, A. (2011). Role of endosomes in simian virus 40 entry and infection. J. Virol. *85*, 4198–4211.

Engering, A., Geijtenbeek, T.B., van Vliet, S.J., Wijers, M., van Liempt, E., Demaurex, N., Lanzavecchia, A., Fransen, J., Figdor, C.G., Piguet, V., and van Kooyk, Y. (2002). The dendritic cell-specific adhesion receptor DC-SIGN internalizes antigen for presentation to T cells. J. Immunol. *168*, 2118–2126.

English, T.J., and Hammer, D.A. (2005). The effect of cellular receptor diffusion on receptor-mediated viral binding using Brownian adhesive dynamics (BRAD) simulations. Biophys. J. *88*, 1666–1675.

Ewers, H., Smith, A.E., Sbalzarini, I.F., Lilie, H., Koumoutsakos, P., and Helenius, A. (2005). Single-particle tracking of murine polyoma virus-like particles on live cells and artificial membranes. Proc. Natl. Acad. Sci. USA *102*, 15110–15115.

Feinberg, H., Guo, Y., Mitchell, D.A., Drickamer, K., and Weis, W.I. (2005). Extended neck regions stabilize tetramers of the receptors DC-SIGN and DC-SIGNR. J. Biol. Chem. *280*, 1327–1335.

Gavrilovskaya, I.N., Shepley, M., Shaw, R., Ginsberg, M.H., and Mackow, E.R. (1998). beta3 Integrins mediate the cellular entry of hantaviruses that cause respiratory failure. Proc. Natl. Acad. Sci. USA *95*, 7074–7079.

Giorgi, C., Accardi, L., Nicoletti, L., Gro, M.C., Takehara, K., Hilditch, C., Morikawa, S., and Bishop, D.H. (1991). Sequences and coding strategies of the S RNAs of Toscana and Rift Valley fever viruses compared to those of Punta Toro, Sicilian Sandfly fever, and Uukuniemi viruses. Virology *180*, 738–753.

Guo, Y., Feinberg, H., Conroy, E., Mitchell, D.A., Alvarez, R., Blixt, O., Taylor, M.E., Weis, W.I., and Drickamer, K. (2004). Structural basis for distinct ligand-binding and targeting properties of the receptors DC-SIGN and DC-SIGNR. Nat. Struct. Mol. Biol. *11*, 591–598.

Johannsdottir, H.K., Mancini, R., Kartenbeck, J., Amato, L., and Helenius, A. (2009). Host cell factors and functions involved in vesicular stomatitis virus entry. J. Virol. *83*, 440–453.

Kuismanen, E., Hedman, K., Saraste, J., and Pettersson, R.F. (1982). Uukuniemi virus maturation: accumulation of virus particles and viral antigens in the Golgi complex. Mol. Cell. Biol. *2*, 1444–1458.

Laughlin, L.W., Meegan, J.M., Strausbaugh, L.J., Morens, D.M., and Watten, R.H. (1979). Epidemic Rift Valley fever in Egypt: observations of the spectrum of human illness. Trans. R. Soc. Trop. Med. Hyg. *73*, 630–633.

Lozach, P.Y., Burleigh, L., Staropoli, I., Navarro-Sanchez, E., Harriague, J., Virelizier, J.L., Rey, F.A., Desprès, P., Arenzana-Seisdedos, F., and Amara, A. (2005). Dendritic cell-specific intercellular adhesion molecule 3-grabbing non-integrin (DC-SIGN)-mediated enhancement of dengue virus infection is independent of DC-SIGN internalization signals. J. Biol. Chem. *280*, 23698–23708.

Lozach, P.Y., Mancini, R., Bitto, D., Meier, R., Oestereich, L., Overby, A.K., Pettersson, R.F., and Helenius, A. (2010). Entry of bunyaviruses into mammalian cells. Cell Host Microbe *7*, 488–499.

Menon, S., Rosenberg, K., Graham, S.A., Ward, E.M., Taylor, M.E., Drickamer, K., and Leckband, D.E. (2009). Binding-site geometry and flexibility in DC-SIGN demonstrated with surface force measurements. Proc. Natl. Acad. Sci. USA *106*, 11524–11529.

Neumann, A.K., Thompson, N.L., and Jacobson, K. (2008). Distribution and lateral mobility of DC-SIGN on immature dendritic cells—implications for pathogen uptake. J. Cell Sci. *121*, 634–643.

Overby, A.K., Pettersson, R.F., Grünewald, K., and Huiskonen, J.T. (2008). Insights into bunyavirus architecture from electron cryotomography of Uukuniemi virus. Proc. Natl. Acad. Sci. USA *105*, 2375–2379.

Pettersson, R., and Kääriäinen, L. (1973). The ribonucleic acids of Uukuniemi virus, a noncubical tick-borne arbovirus. Virology *56*, 608–619.

Peyrefitte, C.N., Perret, M., Garcia, S., Rodrigues, R., Bagnaud, A., Lacote, S., Crance, J.M., Vernet, G., Garin, D., Bouloy, M., and Paranhos-Baccalà, G. (2010). Differential activation profiles of Crimean-Congo hemorrhagic fever virus- and Dugbe virus-infected antigen-presenting cells. J. Gen. Virol. *91*, 189–198.

Raftery, M.J., Kraus, A.A., Ulrich, R., Krüger, D.H., and Schönrich, G. (2002). Hantavirus infection of dendritic cells. J. Virol. *76*, 10724–10733.

Sanchez, A.J., Vincent, M.J., and Nichol, S.T. (2002). Characterization of the glycoproteins of Crimean-Congo hemorrhagic fever virus. J. Virol. *76*, 7263–7275.

Sbalzarini, I.F., and Koumoutsakos, P. (2005). Feature point tracking and trajectory analysis for video imaging in cell biology. J. Struct. Biol. *151*, 182–195.

Schmaljohn, C., and Nichol, S. (2007). Bunyaviridae, K.D. Fields Virology, ed. (Philadelphia: Lippincott Williams & Wilkins), pp. 1741–1788.

Schmaljohn, C.S., Hasty, S.E., Rasmussen, L., and Dalrymple, J.M. (1986). Hantaan virus replication: effects of monensin, tunicamycin and endoglycosidases on the structural glycoproteins. J. Gen. Virol. *67*, 707–717.

Sol-Foulon, N., Moris, A., Nobile, C., Boccaccio, C., Engering, A., Abastado, J.P., Heard, J.M., van Kooyk, Y., and Schwartz, O. (2002). HIV-1 Nef-induced upregulation of DC-SIGN in dendritic cells promotes lymphocyte clustering and viral spread. Immunity *16*, 145–155.

Soldan, S.S., and González-Scarano, F. (2005). Emerging infectious diseases: the Bunyaviridae. J. Neurovirol. *11*, 412–423.

Svajger, U., Anderluh, M., Jeras, M., and Obermajer, N. (2010). C-type lectin DC-SIGN: an adhesion, signalling and antigen-uptake molecule that guides dendritic cells in immunity. Cell. Signal. *22*, 1397–1405.

Tabarani, G., Thépaut, M., Stroebel, D., Ebel, C., Vivès, C., Vachette, P., Durand, D., and Fieschi, F. (2009). DC-SIGN neck domain is a pH-sensor controlling oligomerization: SAXS and hydrodynamic studies of extracellular domain. J. Biol. Chem. *284*, 21229–21240.

van Kooyk, Y. (2008). C-type lectins on dendritic cells: key modulators for the induction of immune responses. Biochem. Soc. Trans. *36*, 1478–1481.